

Photodissociation of LiFH and NaFH van der Waals complexes: A semiclassical trajectory study

Ahren W. Jasper, Michael D. Hack, Arindam Chakraborty, and Donald G. Truhlar^{a)}
Department of Chemistry and Supercomputer Institute, University of Minnesota, Minneapolis, Minnesota 55455

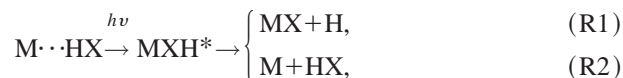
Piotr Piecuch
Department of Chemistry, Michigan State University, East Lansing, Michigan 48824

(Received 21 June 2001; accepted 9 August 2001)

The photodissociation of Li··FH and Na··FH van der Waals complexes is studied using Tully's fewest-switches surface-hopping and the natural decay of mixing semiclassical trajectory methods for coupled-state dynamics. The lifetimes of the predissociated excited-state complex (exciplex), as well as the branching ratio into reactive and nonreactive arrangements and the internal energy distribution of the products are reported at several excitation energies. The semiclassical trajectory methods agree with each other only qualitatively, and the results are strongly dependent on the choice of electronic representation. In general, the lifetime of the LiFH exciplex is shorter and less dependent on the excitation energy than the lifetime of the NaFH exciplex. The semiclassical dynamics of LiFH and NaFH are interpreted in terms of the features of their coupled potential energy surfaces. © 2001 American Institute of Physics. [DOI: 10.1063/1.1407278]

I. INTRODUCTION

There has been recent interest in the transition-state spectroscopy^{1,2} of metal-halide "harpooning"^{3–8} reactions:



where X is a halogen, M is a metal atom, "··" indicates a weak van der Waals interaction, and "*" indicates electronic excitation. These processes provide a means of probing the transition-state of the M* + HX reaction. The excited-state complex (exciplex) that is formed by vertically exciting the system from the van der Waals well is characterized by a relatively deep well in the excited-state (e.g., ~0.5 eV for Na··FH^{9,10}). The long-lived exciplex may decay by one of two pathways. In the "harpooning" process (R1), the change in the electronic state of the system weakens the HX bond and leads to the formation of an MX product. In the competing process (R2), the system relaxes to the ground electronic state by exciting the internal vibrational and rotational modes of HX. In addition, when the excitation energy is high enough, the system may also decay into excited M* and HX.

Here we consider the (R1) and (R2) processes for the cases where M=Li or Na and X=F. Both the potential energy surfaces^{9–25} and dynamics^{18,22–37} of the ground electronic states of the LiFH and NaFH systems have been widely studied. The coupled potential energy surfaces and coupled-state dynamics of LiFH¹⁹ and NaFH^{7,9,10,38} have also been studied in a more limited sense. The NaFH and LiFH systems are similar in many respects to the coupled-state problem in the well-studied LiH₂^{39–42} and NaH₂^{39,43–50} systems, which may be interpreted to a first approximation

by the ionic-covalent intersection model of Magee *et al.*⁵¹ A critical difference though is that LiH₂ and NaH₂ have conical intersections of their adiabatic ground- and excited-state surfaces, whereas LiFH and NaFH have appreciable energy gaps at all geometries.

We have previously presented³⁸ colinear quantum mechanical wave packet and semiclassical trajectory results for the NaFH system. These results show qualitative disagreement between the semiclassical and quantum calculations, presumably due to the deep quantum nature of the electronic transitions in systems with large adiabatic energy gaps. Our group has recently developed several improved methods^{52–54} for simulating processes involving electronic state changes that may be more applicable to large-gap systems. These methods are based on the semiclassical Ehrenfest⁵⁵ method and have the desirable feature that trajectories decohere to a single electronic state in the absence of electronic-state coupling. One of these new methods, namely the natural decay of mixing⁵⁴ (NDM) algorithm, is general enough to treat photodissociation, and we will apply this method to the photodissociation of Li··FH and Na··FH in the present paper. For comparison we also consider the fewest-switches⁵⁶ surface-hopping^{56–70} scheme suggested by Tully.

In this article we report fully three-dimensional semiclassical dynamics calculations in which we modeled the photodissociation of the LiFH and NaFH systems using the NDM self-consistent potential method and Tully's fewest-switches (TFS) surface-hopping method. Both methods may be formulated in terms of the adiabatic or the diabatic representations. It has been suggested⁷⁰ that the adiabatic representation should always be preferred, although we have found that in some cases more accurate results are obtained using the diabatic electronic states.⁷¹ In the present work, we find that surface-hopping is more sensitive to the choice of

^{a)}Electronic mail: truhlar@umn.edu

TABLE I. Geometries and energies of the adiabatic stationary points of LiFH and NaFH. All bond lengths are in bohr, the M-F-H angle θ is in degrees, and the energies are in eV.

LiFH features	r_{LiF}	r_{HF}	r_{LiH}	θ_{LiFH}	V_1	$V_1 + \text{ZPE}^a$	V_2	$V_2 + \text{ZPE}^a$
Reactants	-	1.73	-	-	0.000	0.251 (0.249)	1.848	2.099 (2.097)
Reactant vdW well of V_1	3.56	1.75	4.48	110.	-0.211	0.096 (0.094)	1.204	-
Saddle point ^b of V_1	3.16	2.43	3.37	72.3	0.352	0.402 (0.402)	2.798	-
Product vdW well of V_1	2.99	3.33	4.67	69.7	0.214	0.287 (0.287)	5.441	-
Products	2.96	-	-	-	0.213	0.260 (0.260)	^c	-
Exciplex of V_2	3.33	1.82	4.70	129.	-0.143	-	1.165	1.396 (1.394)
NaFH features ^d	r_{NaF}	r_{HF}	r_{NaH}	θ_{NaFH}	V_1	$V_1 + \text{ZPE}^a$	V_2	$V_2 + \text{ZPE}^a$
Reactants	-	1.73	-	-	0.000	0.251 (0.249)	2.097	2.342 (2.346)
Reactant vdW well of V_1	4.68	1.74	1.11	118.	-0.074	0.351 (0.352)	2.031	-
Saddle point ^e of V_1	3.66	3.49	1.11	90.8	1.270	1.299 (1.299)	5.622	-
Products	3.64	-	-	-	1.182	1.218 (1.220)	^c	-
Exciplex of V_2	4.17	1.83	1.11	117.	0.020	-	1.600	1.911 (1.909)

^aThe zero point energy (ZPE) was calculated treating the normal modes as separable harmonic oscillators (Ref. 94) using the POLYRATE *v*.8.5.1 software package (Ref. 95). Values in parentheses were obtained by using the Morse I approximation (Ref. 96) to include anharmonicity in the stretches. Zero point energy is included in one mode for reactants and products, in the two bound modes for the saddle points, and in three modes for the three-body local minima.

^bImaginary frequency: 1480i cm^{-1} .

^cThe product arrangement is not bound on the excited-state surface V_2 .

^dThe NaFH surface does not support a product van der Waals well.

^eImaginary frequency: 1650i cm^{-1} .

electronic representation than the NDM method. The results of the NDM and TFS methods agree with each other only qualitatively, and we discuss the differences in terms of the problem of frustrated hopping^{69,72} that plagues most TFS calculations. The dynamics of LiFH is also compared to that of NaFH and interpreted in terms of the features of the LiFH and NaFH coupled potential energy surfaces.

The calculations on NaFH employ an improved version of a set of coupled potential energy surfaces presented previously,¹⁰ and the calculations on LiFH employ a new set of coupled potential energy surfaces described briefly in Sec. II A. In Sec. II B we present the improved potential energy surfaces for NaFH. In Sec. III we present the dynamics calculations. Sections IV and V contain the results and discussion, and in Sec. VI we give a brief summary.

II. LiFH AND NaFH POTENTIAL ENERGY SURFACES

II. A. LiFH potential energy surfaces

We have performed high-level *ab initio* calculations for the two lowest-energy adiabatic states of LiFH. The electronic structure calculations used in the present work are a subset of the calculations that will be presented in more detail in a future publication.⁷³ For the present work, more than 4000 calculations were performed over a dense grid of nuclear geometries using the MRDCI variant of the multireference configuration interaction method.^{74–76} Specifically, the HF internuclear distance was varied from 1.2–7.0 bohr, and the LiF internuclear distance was varied from 2.0 to 15 bohr. This two-dimensional grid was repeated at five Li–F–H bond angles: 45, 70, 90, 110, and 179.99°. Additional points were calculated for other Li–F–H angles including 0.01, 130, and 150°. The resulting dense grid of adiabatic energies was used to develop a coupled set of analytic potential energy surfaces for the two lowest-energy electronic states, as discussed next.

Coupled potential energy surfaces may be expressed in either the adiabatic or the diabatic representation. We fit the LiFH surfaces in the diabatic (more precisely, quasidiabatic^{77–89}) representation, because the coupling between quasidiabatic states is scalar, whereas the coupling between adiabatic states is a vector quantity and hence requires more analytic functions to represent. The quasidiabatic surfaces have the additional advantage that they are typically smoother functions of geometry than the adiabatic surfaces, and therefore require less complicated functional forms. The quasidiabatic potential energy matrix \mathbf{U} consists of the potential energy surfaces U_{11} and U_{22} and their scalar coupling $U_{12} = U_{21}$. The matrix \mathbf{U} can be diagonalized to recover the adiabatic surfaces V_1 and V_2 , and we can also obtain the nonadiabatic coupling (i.e., the nuclear–momentum coupling that couples motion on the adiabatic surfaces) analytically from the quasidiabatic energies and their gradients.⁹⁰

The analytic matrix \mathbf{U} was obtained by developing physically-motivated functional forms for the individual matrix elements, and flexibility in the fit was achieved by introducing more than 80 adjustable parameters. These parameters were optimized using a genetic algorithm⁹¹ such that the RMS deviation of the adiabatic energies V_1 and V_2 from the *ab initio* data was minimized and such that U_{12} vanishes in all asymptotic regions (i.e., in regions where one atom is infinitely far from the other two). Critical regions of the surface (e.g., the van der Waals well) were weighted more than less important regions (e.g., high-energy regions) to obtain the final values of the parameters. Details of the functional forms and parameters of the analytic LiFH fit are given in the supporting information.⁹² The geometries and energies of the stationary points of the analytic LiFH surfaces are shown in Table I. The potential energy surfaces along the minimum energy path of the ground-state reaction are plotted in Fig. 1.

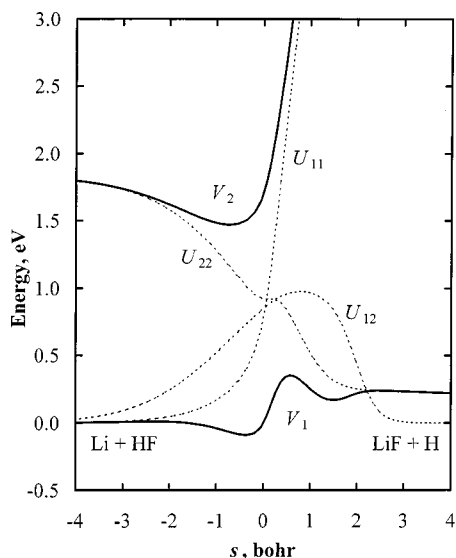


FIG. 1. Adiabatic (thick solid lines) and quasidiabatic (thin dashed lines) energies along the ground-state reaction coordinate s for $\text{Li}+\text{HF}\rightarrow\text{LiF}+\text{H}$ at a fixed bond angle of 72° .

II. B. NaFH potential energy surfaces

We have previously presented an analytic fit¹⁰ for the two lowest-energy electronic states of NaFH (which we will call surface set NaFH-A) based on high-level *ab initio* (MRDCI) calculations. The surface set was shown to be quantitatively accurate in the interaction region and was successfully used to reproduce the experimental photodepletion spectrum of the NaFH van der Waals system.⁷ In the current work we use an improved version of the previous fit which we will call surface set NaFH-B. The new fit includes better representations of the experimental diatomic curves for HF and NaF in the asymptotic regions and features a localized diabatic coupling that vanishes in all asymptotic regions. The NaFH-B fit was obtained by adding a correction function to the diagonal quasidiabatic surfaces U_{11} and U_{22} and cutting off the scalar coupling U_{12} . Details of the functional forms of the new fit are given in the supporting information.⁹² The geometries and energies of the stationary points are shown in Table I. The potential energy surfaces along the minimum energy path of the ground-state reaction for the surface set NaFH-B are shown in Fig. 2.

III. SEMICLASSICAL TRAJECTORY CALCULATIONS

We performed a series of semiclassical trajectory calculations simulating the photodissociation processes (R1) and (R2) using the LiFH and NaFH-B quasidiabatic potential energy matrices. The semiclassical trajectory calculations were carried out using version 6.4 of the NAT computer code.⁹³ Each simulation included an ensemble of 3000 trajectories.

The initial conditions for a given trajectory in each ensemble were selected according to the following prescription: (1) The initial position and momentum of the trajectory were selected from a distribution corresponding to the non-rotating ground vibrational state in the electronically adiabatic ground-state van der Waals well. Specifically, the three Jacobi coordinates of the system (the HF stretch r , the

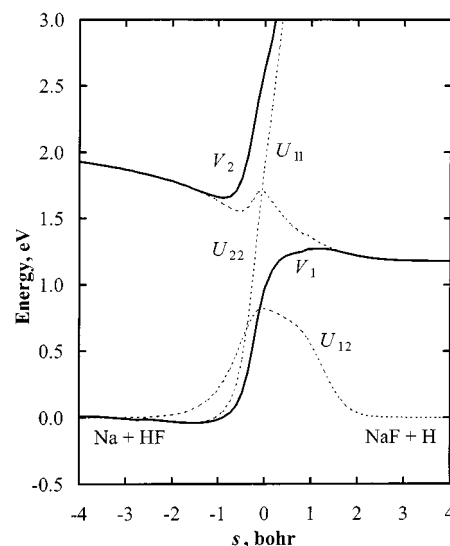


FIG. 2. Adiabatic (thick solid lines) and quasidiabatic (thin dashed lines) energies along the ground-state reaction coordinate s for $\text{Na}+\text{HF}\rightarrow\text{NaF}+\text{H}$ at a fixed bond angle of 91° .

M-[HF] stretch R , and the M-[HF] bend χ , where [HF] indicates the center of mass of HF) at the minimum of the van der Waals complex were assumed to be separable, and each trajectory was given the appropriate zero point energy (obtained from one-dimensional Morse fits to the potential energy along r , R , and χ) in each mode and a random phase. (2) After assigning the initial geometry \mathbf{R}_0 and momentum as described, the trajectories were immediately excited into the excited adiabatic state with an energy $h\nu$. If the difference between the adiabatic energy gap of the electronic states at \mathbf{R}_0 and the excitation energy $h\nu$ was not within some specified tolerance ε , the excitation was rejected, and step (1) was repeated. The tolerance ε used for all of the runs reported here was 0.01 eV. Calculations were performed with excitation energies $h\nu$ equal to 1.5, 1.6, 1.7, 1.8, and 1.9 eV.

The energy of the ground vibrational state in the separable Jacobi approximation is 0.065 and 0.19 eV for $\text{Li}\cdot\cdot\text{FH}$ and $\text{Na}\cdot\cdot\text{FH}$, respectively. (These values were obtained by adding the zero point energies of 0.28 and 0.27 eV to well energies of -0.21 and -0.074 eV, respectively.) Note that these energies differ from those reported in Table I, because the values in Table I are estimated using separable normal modes⁹⁴⁻⁹⁶ (and are therefore our best estimate), whereas our semiclassical trajectory code requires the zero point energy expressed in terms of separable r , R , and χ motions. The total energy of the semiclassical trajectories ranges from approximately 1.6 to 2.0 eV for LiFH and from approximately 1.7 to 2.1 eV for NaFH. The zero of energy is defined as Li or Na infinitely far from HF at its equilibrium internuclear bond distance.

We used two different semiclassical trajectory methods for coupled-states dynamics: Tully's fewest-switches⁵⁶ (TFS) method and the natural decay of mixing⁵⁴ (NDM) method. The TFS method belongs to the general class of surface-hopping methods where each trajectory in the ensemble is propagated under the influence of a single potential energy surface and propagation is interrupted by instantaneous sur-

face transitions according to a fewest-switches algorithm. A corresponding kinetic energy adjustment is made along the nonadiabatic coupling vector such that the total energy is conserved. For the calculations reported here, classically forbidden electronic transitions were ignored. We performed TFS calculations in both the adiabatic (TFSa) and quasidiabatic (TFSd) representations.

The NDM method⁵⁴ is a modification of the Ehrenfest self-consistent potential method that incorporates decoherence into the equations for the electronic motion and thereby produces trajectories that finish the simulation in a pure electronic state. When the surfaces are strongly coupled, NDM trajectories evolve on an average potential energy surface similar to the Ehrenfest potential energy surface. As the coupling between the electronic surfaces decreases to zero, the electronic density matrix gradually collapses to the diagonal form that corresponds to propagation in a single electronic state. We performed calculations in both the adiabatic (NDMa) and quasidiabatic (NDMd) representations. The NDM method has previously only been discussed in terms of the diabatic representation; we discuss the NDMa method in the Appendix.

As discussed above, the initial conditions were selected using the adiabatic potential energy surfaces, independent of the representation used for propagation. For NDMd runs, the initial electronic state was transformed from the adiabatic to the quasidiabatic representation before propagation as discussed previously.⁵⁴ For the TFSd runs, the electronic representation transformation was performed as follows. The excited adiabatic state may be expressed as a linear combination of the two quasidiabatic electronic states. The initial quasidiabatic state for a TFSd run was selected randomly with a probability given by the square of the corresponding expansion coefficient. In general, the state that is selected as the initial quasidiabatic state will not have the same potential energy as the initial adiabatic state. In order to compensate for the change in the potential energy, the nuclear momentum was scaled such that the total energy was conserved and the direction of the nuclear momentum was unchanged.

Trajectories were propagated until the resulting products were dissociated by at least 15 bohr. The product branching ratios were computed by counting the trajectories that finish in each of the two final product arrangements. We refer to the M+FH product arrangement as the “quenching” process and the MF+H arrangement as the “reactive” process, although they may be more accurately described as nonreactive deexcitation and reactive deexcitation, respectively. These nonadiabatic probabilities are labeled P_Q and P_R , respectively. Trajectories may also dissociate into reactants in an excited electronic state ($M^* + HF$) at excitation energies $h\nu$ of 1.78 eV for the LiFH system and 1.91 eV for the NaFH system. (These excitation energies correspond to 1.85 and 2.10 eV for the $Li \rightarrow Li^*$ and $Na \rightarrow Na^*$ excitations, respectively. Note that classical trajectories may dissociate without the required zero point energy in HF.) Even when energetically allowed, the probability of this process is small (much less than 0.01), and we will not consider unquenched trajectories in the present work.

For both quenching and reactive trajectories, we computed the final vibrational ($\langle \nu' \rangle$ and $\langle \nu'' \rangle$) and rotational ($\langle j' \rangle$ and $\langle j'' \rangle$) moments (i.e., averages), where the single and double primes refer to reactive and quenching trajectories, respectively. The moments were calculated using the energy-nonconserving histogram (ENH) method, as described elsewhere.⁹⁷ We verified that using the energy-nonconserving quadratic- and linear-smooth sampling schemes and the energy-conserving variants of all three sampling schemes give results that are within the statistical uncertainties reported for the ENH results.

The lifetime of the exciplex was computed as follows: The delay time T_d for each trajectory in the ensemble was calculated from the total simulation time T , the final relative velocity $\nu_R(T)$, and the final translational Jacobi atom-diatom distance $R(T)$:

$$T_d = T - \nu_R(T)/R(T). \quad (1)$$

The second term in Eq. (1) makes the result be independent of the arbitrary stopping time T . Trajectories with the delay times greater than T_d^{\max} or less than T_d^{\min} were excluded, and the remaining delay times were binned. The resulting curve, which represents the probability that the system has not dissociated from the exciplex as a function of time, was fit to the exponential

$$P(T_d) = A \exp(-T_d/\tau), \quad (2)$$

where τ is the lifetime of the exciplex, and A is a fitting parameter. The parameters T_d^{\max} and T_d^{\min} were chosen such that $\sim 20\%$ of trajectories were excluded by each cut-off parameter, i.e., the middle 60% of delay times were considered. The number of bins was typically 80–100. The calculated lifetimes were found to vary only slightly with small changes in the number of bins and the cut-off parameters T_d^{\max} and T_d^{\min} .

Note that one could also define the delay time for a photodissociation process as

$$T_d = T - \nu_R(T)/[R(T) - R(0)], \quad (3)$$

where $R(0)$ is the initial translational Jacobi distance. We verified that the differences in the lifetimes obtained by using Eqs. (1) and (3) were smaller than the estimated statistical uncertainties, and we report only the lifetimes calculated with Eq. (1).

IV. RESULTS

Tables II and III present the lifetimes, product branching probabilities, and final vibrational and rotational moments for the NaFH and LiFH systems. The observables are reported as a function of the excitation energy $h\nu$ for the both TFS and NDM semiclassical trajectory methods in both the adiabatic and quasidiabatic electronic representations. The relative uncertainties in the reactive and quenching moments are typically 2% and 4%, respectively, and the uncertainty in the probabilities is typically 0.01. The dominant uncertainty in the lifetimes is due to the choice of the cut-off parameters T_d^{\max} and T_d^{\min} , and we estimate the relative uncertainty in the lifetimes to be between 5% and 10%.

TABLE II. Lifetimes, branching ratios, and final vibrational and rotational moments for NaFH.

Method	$h\nu$ (eV)	τ (ps)	P_R	$\langle \nu' \rangle$	$\langle j' \rangle$	P_Q	$\langle \nu'' \rangle$	$\langle j'' \rangle$
NDMa	1.5	21.	0.81	2.76	10.6	0.19	1.79	6.2
	1.6	7.8	0.80	3.19	12.8	0.20	1.49	8.0
	1.7	3.3	0.76	3.11	14.2	0.24	1.56	7.6
	1.8	1.6	0.83	3.07	13.8	0.17	1.58	8.4
	1.9	0.68	0.82	3.04	15.6	0.18	1.70	8.6
TFSa	1.5	11.	0.96	2.74	11.9	0.04	1.63	8.6
	1.6	4.8	0.90	2.93	11.5	0.11	1.61	9.5
	1.7	3.0	0.88	3.50	12.5	0.12	1.47	10.6
	1.8	1.6	0.90	3.79	13.3	0.10	1.59	11.8
	1.9	0.88	0.88	4.67	14.0	0.11	1.67	12.0
NDMd	1.5	0.57	0.37	1.93	10.3	0.63	1.17	5.2
	1.6	0.40	0.33	2.39	12.9	0.67	0.91	8.7
	1.7	0.32	0.34	2.99	15.0	0.66	0.88	8.6
	1.8	0.26	0.55	3.75	14.5	0.45	0.92	9.1
	1.9	0.24	0.56	4.11	18.3	0.44	1.25	9.2
TFSd	1.5	0.26	0.22	0.63	13.4	0.79	2.34	2.5
	1.6	0.19	0.51	0.80	13.7	0.49	2.04	4.3
	1.7	0.17	0.63	1.54	14.1	0.38	1.84	5.6
	1.8	0.10	0.81	3.09	14.7	0.19	1.86	5.9
	1.9	0.027	0.87	4.93	14.6	0.12	1.81	8.5

The four semiclassical trajectory methods predict the same trends in the lifetimes, as shown in Fig. 3. Specifically, the lifetime of the LiFH exciplex is shorter and less dependent on energy than that of the NaFH exciplex. The lifetime of LiFH increases as a function of the excitation energy by a factor of 1.2 to 2.5 over the range of energies studied, whereas the lifetime of NaFH decreases. The relative decrease in the lifetime of NaFH is greater for the adiabatic methods (factors of 34 and 13) than for the quasidiabatic methods (factors of 9.8 and 2.4). The lifetimes of the LiFH exciplex calculated by the NDM method are relatively independent of the choice of electronic representation, whereas the TFSa method predicts lifetimes slightly greater than

TABLE III. Lifetimes, branching ratios, and final vibrational and rotational moments for LiFH.

Method	$h\nu$ (eV)	τ (ps)	P_R	$\langle \nu' \rangle$	$\langle j' \rangle$	P_Q	$\langle \nu'' \rangle$	$\langle j'' \rangle$
NDMa	1.5	0.094	0.90	2.87	11.3	0.10	1.51	5.9
	1.6	0.13	0.89	3.25	14.5	0.11	1.31	8.6
	1.7	0.13	0.87	3.89	13.0	0.13	1.61	7.3
	1.8	0.14	0.89	4.10	14.6	0.11	1.55	7.9
	1.9	0.11	0.94	3.65	17.4	0.06	1.37	14.1
TFSa	1.5	0.15	0.98	2.56	9.0	0.02	1.76	8.7
	1.6	0.21	0.95	3.31	12.2	0.05	1.94	7.9
	1.7	0.26	0.91	3.86	13.8	0.09	2.02	9.2
	1.8	0.28	0.90	4.16	16.6	0.10	1.93	10.7
	1.9	0.28	0.82	4.15	18.1	0.09	1.85	12.1
NDMd	1.5	0.061	0.88	3.19	13.1	0.12	0.94	7.5
	1.6	0.095	0.81	3.12	19.6	0.19	0.88	10.1
	1.7	0.13	0.69	3.17	20.3	0.31	0.98	10.7
	1.8	0.14	0.64	3.42	19.1	0.36	0.87	13.3
	1.9	0.15	0.65	3.33	19.9	0.34	0.74	17.0
TFSd	1.5	0.015	0.93	4.58	7.8	0.07	1.32	6.0
	1.6	0.026	0.90	4.80	8.4	0.10	1.45	6.9
	1.7	0.029	0.89	5.10	7.7	0.11	1.32	7.8
	1.8	0.030	0.89	6.14	6.5	0.11	1.36	7.8
	1.9	0.036	0.89	6.26	6.7	0.10	1.51	8.8

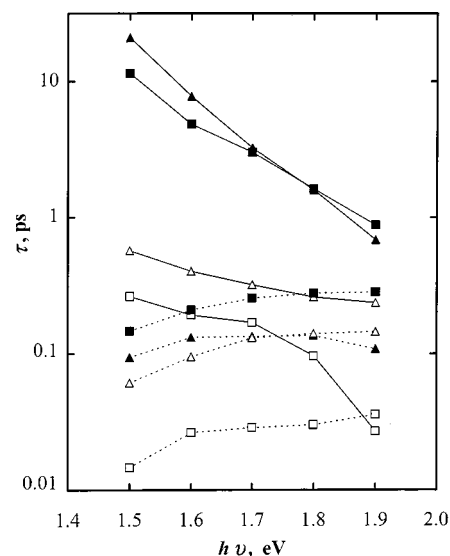


FIG. 3. Lifetime τ of the LiFH exciplex (dashed lines) and NaFH exciplex (solid line) as a function of excitation energy $h\nu$. Solid squares represent the TFSa method, open squares represent the TFSd method, solid triangles represent the NDMa method, and open triangles represent the NDMd method. Note that the ordinate scale is logarithmic.

those of the NDM methods, and the TFSd method predicts shorter lifetimes by a factor of 2 to 4. The agreement between the adiabatic and diabatic methods is worse for the NaFH system, where the results vary, on average, by a factor of 16 for the NDM methods and 21 for the TFS methods. In all cases except one, the diabatic methods predict shorter lifetimes, and the agreement between the two electronic representations usually improves as the excitation energy decreases.

Although the magnitudes vary significantly among the methods, the reactive quenching process is usually preferred, and the probability of reaction P_R is usually greater for the LiFH system than for the NaFH system. For the adiabatic methods, P_R is generally constant as a function of energy for both the NaFH and LiFH systems. There is a greater variation of P_R with energy in the diabatic results, especially for the NaFH system. The magnitude of P_R is usually in the range of 0.70 to 0.90 except for the diabatic results for the NaFH system, where P_R is as low as 0.22 for TFSd and does not exceed 0.56 for NDMd.

The final vibrational and rotational moments show no clear trend as a function of energy, and the magnitudes vary significantly between the semiclassical trajectory methods. The NDMa and TFSa methods qualitatively agree with each other, whereas the NDMd and TFSd methods exhibit a larger discrepancy.

V. DISCUSSION

The excitation energy of Li (1.85 eV) is lower than that of Na (2.10 eV) by 0.25 eV. This, combined with the fact that the product LiF+H valley is lower in energy than the NaF+H product valley, results in an adiabatic energy gap that is typically smaller in the LiFH system. In Fig. 4, we show contour plots of the adiabatic energy gap ($V_2 - V_1$) for the colinear LiFH and NaFH systems. Also shown is the

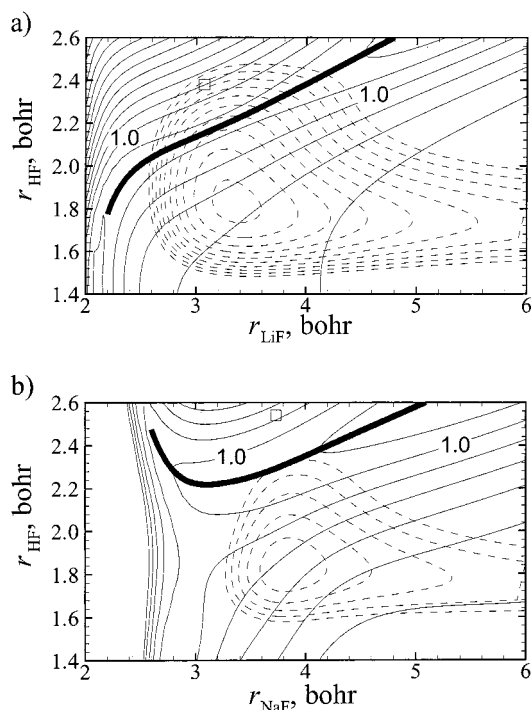


FIG. 4. Adiabatic energy gap for (a) the LiFH system and (b) the NaFH system. The bond angle is fixed at 180° . The solid contours represent the adiabatic energy gap ($V_2 - V_1$), where the minimum contour is 0.6 eV for LiFH and 0.8 eV for NaFH, and the contour spacing is 0.2 eV. The 1.0 eV contours are labeled in both cases. The dashed contours show the exciplex wells, where the highest energy contour is 2.1 eV and the contour spacing is 0.1 eV. The line of avoided crossings of V_1 and V_2 (where U_{11} and U_{22} cross) is shown as a thick solid line, and the saddle point on the ground electronic surface is indicated by the square.

exciplex well, the line of avoided crossings, and the location of the saddle point on the ground electronic surface at colinear geometries. For LiFH, the smallest energetically accessible adiabatic energy gap for the excitation energies studied here is approximately 0.8 eV, and the line of the smallest energy gap passes near the minimum of the exciplex well. Electronic transitions are promoted near the line of minimum energy gaps, and we therefore observe LiFH lifetimes that are short and relatively independent of the total energy of the system. The energetically accessible minimum energy gap for NaFH, on the other hand, varies from about 0.9 to 1.2 eV as a function of the excitation energy, and the line of avoided crossing is farther from the minimum of the exciplex well in the NaFH system than in the LiFH system. We therefore observe NaFH complexes with long lifetimes that are strongly dependent on the excitation energy.

We have previously introduced and discussed several criteria for estimating the most accurate electronic representation for surface-hopping.⁷¹ We concluded that the representation that minimizes the number of attempted hops (and is therefore the representation in which the states of the system are the least coupled) is the preferred electronic representation for surface-hopping, and we call this the Calaveras Co. (CC) representation. For both the LiFH and NaFH systems, the CC representation is the adiabatic representation. The rationale for preferring the CC representation is closely re-

lated to the problem of frustrated hops.⁷¹ For the LiFH and NaFH systems, frustrated hopping occurs in nearly every one of the TFSd trajectories, whereas only 60% of TFSa trajectories experience a frustrated hop. The breakdown of the TFS algorithm leads to a decrease in the lifetimes, and we observe that the TFSd method predicts smaller lifetimes than the TFSa method. We can also assume that the TFSa method is predicting lifetimes that are too short due to the presence of frustrated hops in the adiabatic calculations.

Frustrated hops destroy the self-consistency of the trajectories and the electronic density matrix, but these remain fully self-consistent in the NDM method. It is encouraging that the NDM results are less sensitive to the choice of electronic representation than are the TFS results. The lifetimes predicted by the NDM method are largely independent of the electronic representation for the LiFH system, but there is some dependence for the NaFH system. We note that when the decoherence time is infinitely large, the nuclear and electronic motion is independent of electronic representation, and that the NDM decoherence time is inversely proportional to the adiabatic energy gap for NDMa and the diabatic energy gap for NDMd. As discussed above, the LiFH system has a smaller energy gap than the NaFH system, and we therefore expect the results for the LiFH system to be less dependent on the choice of electronic representation. We also note that the definition of the decoherence time in the NDM method is somewhat arbitrary. More sophisticated forms of the decoherence time could be introduced (perhaps the simplest of which would be to introduce a multiplicative prefactor that is greater than one) such that the dependence of the NDM results on the choice of electronic representation is reduced for large-gap systems.

Physically, the line of avoided crossings (where $U_{11} = U_{22}$) corresponds to a change in the valence-bond character of the adiabatic state and is in the center of the region where electronic transitions are most likely to occur. From Fig. 4 we see that in the energetically accessible regions of the excited electronic state, the LiFH exciplex is more readily able to access the seam than is the NaFH exciplex. We also note that in the LiFH system, electronic transitions are likely to occur closer to the saddle point than for the NaFH system. In fact, the well on the upper surface of the LiFH system stretches to the region of the saddle point on the ground-state surface. This is not the case for NaFH. In addition, the height of the reaction barrier for LiFH is much smaller than for NaFH. Therefore, we expect LiF to form more readily than NaF for a given total energy, and this trend is observed in the results of the semiclassical trajectory calculations.

VI. SUMMARY

We have performed a set of semiclassical trajectory calculations for the photodissociation of LiFH and NaFH. The calculations were performed with two different methods for nonadiabatic dynamics and in both the adiabatic and diabatic representations. Although the results using various methods and representations are not in quantitative agreement with each other, several clear trends emerge. Specifically, the lifetime of the NaFH complex decreases with increasing excita-

tion energy and is strongly dependent on the excitation energy. The lifetime of the LiFH complex, on the other hand, is shorter than the lifetime of the NaFH complex and is less dependent on the excitation energy. The LiFH system is also found to be more reactive than the NaFH system at similar excitation energies. We have explained these results by considering the features of the coupled potential energy surfaces of the LiFH and NaFH systems.

Experiments on these systems are underway in the laboratory of Professor John Polanyi, and our calculations are stimulated by the hope that calculations such as those reported here can eventually be compared to experiment.

ACKNOWLEDGMENTS

This work was supported in part by the National Science Foundation under Grant No. CHE00-92019 and by the Michigan State University Intramural Research Grant Program. The authors are grateful to Rudolf Burcl, Xiao Yan Chang, Andrew Hudson, Gil Kätz, Ronnie Kosloff, Han-Bin Oh, John Polanyi, Vladimir Špirko, and Yehuda Zeiri for many helpful interactions.

APPENDIX: NATURAL DECAY OF MIXING IN THE ADIABATIC REPRESENTATION

The NDM method was initially presented⁵⁴ in the diabatic representation, and here we present the details of the NDMA method. We will consider a two-state system where the electronic wave function is given by

$$\Psi = c_1 \phi_1 + c_2 \phi_2, \quad (\text{A1})$$

ϕ_k are the adiabatic electronic basis functions, and c_k are the complex expansion coefficients,

$$c_k = \frac{1}{\sqrt{2}}(x_k + ip_k). \quad (\text{A2})$$

The NDMA expressions for the rate of change of the real and imaginary parts of c_k are

$$\dot{x}_k = \dot{x}_k^E + \dot{x}_k^D, \quad (\text{A3})$$

$$\dot{p}_k = \dot{p}_k^E + \dot{p}_k^D, \quad (\text{A4})$$

where the superscript "E" denotes the usual Ehrenfest⁵⁵ electronic dynamics. The additional decoherence terms are given by

$$\dot{x}_k^D = (1 - \delta_{kK}) \left(-\frac{1}{2} \frac{x_k}{\tau_{kK}} \right) + \delta_{kK} \frac{1}{2} \frac{x_k}{|c_k|^2} \sum_{k' \neq k} \frac{|c_{k'}|^2}{\tau_{kk'}}, \quad (\text{A5})$$

$$\dot{p}_k^D = (1 - \delta_{kK}) \left(-\frac{1}{2} \frac{p_k}{\tau_{kK}} \right) + \delta_{kK} \frac{1}{2} \frac{p_k}{|c_k|^2} \sum_{k' \neq k} \frac{|c_{k'}|^2}{\tau_{kk'}}, \quad (\text{A6})$$

where K is the state towards which the system is decohering,

$$\tau_{ik} = \frac{\hbar}{|V_i - V_k|} \frac{E}{T_{\text{vib}}}, \quad (\text{A7})$$

E is the total energy of the system, V_k is the adiabatic energy of state k , and T_{vib} is the vibrational energy, as described

elsewhere.⁵⁴ The decoherent state K is selected using the fewest-switches criterion and the adiabatic electronic states. See Ref. 54 for details.

We note that the Ehrenfest expressions that appear in Eqs. (A3) and (A4) can in principle be integrated in either representation for the NDMA method, but the expressions are much easier to integrate in the diabatic representation. In our implementation of the NDMA method, the decoherence terms are calculated from Eqs. (A5) and (A6) and transformed to the diabatic representation before being added to the diabatic Ehrenfest terms for propagation.

¹P. R. Brooks, Chem. Rev. **88**, 407 (1988).

²J. C. Polanyi and A. H. Zewail, Acc. Chem. Res. **29**, 119 (1995).

³M. Polanyi, *Atomic Reactions* (Williams and Norgate, London, 1932).

⁴D. R. Herschbach, *Advances in Chemical Physics*, edited by J. Ross (Interscience, New York, 1966), Vol. 10, p. 319.

⁵R. D. Levine and R. B. Bernstein, *Molecular Reaction Dynamics and Chemical Reactivity* (Oxford University Press, New York, 1987), pp. 134ff.

⁶X.-Y. Chang, R. Ehlich, A. J. Hudson, P. Piecuch, and J. C. Polanyi, Faraday Discuss. Chem. Soc. **108**, 411 (1997).

⁷M. S. Topaler, D. G. Truhlar, X. Y. Chang, P. Piecuch, and J. C. Polanyi, J. Chem. Phys. **108**, 5378 (1998).

⁸A. J. Hudson, H. B. Oh, J. C. Polanyi, and P. Piecuch, J. Chem. Phys. **113**, 9897 (2000); A. J. Hudson and J. C. Polanyi (personal communication).

⁹A. Sevin, P. C. Hilbert, and J.-M. Lefour, J. Am. Chem. Soc. **109**, 1845 (1987).

¹⁰M. S. Topaler, D. G. Truhlar, X. Y. Chang, P. Piecuch, and J. C. Polanyi, J. Chem. Phys. **108**, 5349 (1998).

¹¹W. A. Lester, Jr. and M. Krauss, J. Chem. Phys. **52**, 4775 (1970).

¹²G. G. Balint-Kurti and R. N. Yardley, Faraday Discuss. Chem. Soc. **62**, 77 (1977).

¹³Y. Zeiri and M. Shapiro, Chem. Phys. **31**, 217 (1978); M. Shapiro and Y. Zeiri, J. Chem. Phys. **70**, 5264 (1979).

¹⁴M. M. L. Chen and H. F. Schaefer III, J. Chem. Phys. **72**, 4376 (1980).

¹⁵S. Carter and J. N. Murrell, Mol. Phys. **41**, 567 (1980).

¹⁶A. Laganà and E. Garcia, THEOCHEM **16**, 91 (1984); E. Garcia and A. Laganà, Mol. Phys. **52**, 1115 (1984); V. Aquilanti, A. Laganà, and R. D. Levine, Chem. Phys. Lett. **158**, 87 (1989); A. Laganà, G. O. d. Aspuru, and E. Garcia, J. Chem. Phys. **108**, 3886 (1998).

¹⁷M. Paniagua, J. M. Garcia de la Vega, J. R. Alvarez Collado, J. C. Sanz, J. M. Alvarino, and A. Laganà, J. Mol. Struct. **142**, 525 (1986).

¹⁸A. Laganà, O. Gervasi, and E. Garcia, Chem. Phys. Lett. **143**, 174 (1988).

¹⁹M. Paniagua and A. Aguado, Chem. Phys. **134**, 287 (1989); A. Aguado and M. Paniagua, J. Chem. Phys. **96**, 1265 (1992); C. Suárez, A. Aguado, and M. Paniagua, Chem. Phys. **178**, 357 (1993); C. Suárez, A. Aguado, C. Tablero, and M. Paniagua, Int. J. Quantum Chem. **52**, 935 (1994); A. Aguado, C. Suárez, and M. Paniagua, Chem. Phys. **201**, 107 (1995).

²⁰A. Laganà, M. L. Hernandez, J. M. Alvarino, L. Castro, and P. Palmieri, Chem. Phys. Lett. **202**, 284 (1993).

²¹O. N. Ventura, Mol. Phys. **89**, 1851 (1996).

²²G. A. Parker, A. Laganà, S. Crocchianti, and R. T. Pack, J. Chem. Phys. **102**, 1238 (1995).

²³A. Aguado, M. Paniagua, M. Lara, and O. Roncero, J. Chem. Phys. **106**, 1013 (1997); **107**, 10085 (1997).

²⁴A. Laganà, J. M. Alvarino, M. L. Hernandez, P. Palmieri, E. Garcia, and T. Martinez, J. Chem. Phys. **106**, 10222 (1997).

²⁵R. Burcl, P. Piecuch, V. Špirko, and O. Bludský, Int. J. Quantum Chem. **80**, 916 (2000); V. Špirko, P. Piecuch, and O. Bludský, J. Chem. Phys. **112**, 189 (2000); F. Mrugała, P. Piecuch, V. Špirko, and O. Bludský, J. Mol. Struct. **555**, 43 (2000).

²⁶C. H. Becker, P. Casauccchia, P. W. Tiedeman, J. J. Valentini, and Y. T. Lee, J. Chem. Phys. **73**, 2833 (1980).

²⁷R. B. Walker, Y. Zeiri, and M. Shapiro, J. Chem. Phys. **74**, 1763 (1981).

²⁸J. M. Alvarino, M. L. Hernandez, E. Garcia, and A. Laganà, J. Chem. Phys. **84**, 3059 (1986); A. Laganà, E. Garcia, and O. Gervasi, *ibid.* **89**, 7238 (1988); A. Laganà, X. Giménez, E. Garcia, and O. Gervasi, Chem. Phys. Lett. **176**, 280 (1991); A. Laganà, G. O. d. Aspuru, A. Aguilar, X. Giménez, and J. M. Lucas, J. Phys. Chem. **99**, 11696 (1995); J. M. Alvarino, V. Aquilanti, S. Cavalli, S. Crocchianti, A. Laganà, and T. Martinez,

- J. Chem. Phys. **107**, 3339 (1997); A. Laganà, A. Bologna, and S. Crocchianti, Phys. Chem. Chem. Phys. **2**, 535 (2000).
- ²⁹M. Hoffmeister, R. Schleysing, F. Steinkemeier, and H. J. Loesch, J. Chem. Phys. **90**, 3528 (1989); H. J. Loesch, E. Stenzel, and B. Wüstenbecker, *ibid.* **95**, 3841 (1991); H. J. Loesch and F. Steinkemeier, *ibid.* **98**, 9570 (1993), **99**, 9598 (1993); H. J. Loesch, A. Ramscheid, E. Stenzel, F. Stienkemeier, and B. Wüstenbecker, in *Physics of Electronic and Atomic Collisions*, edited by W. R. MacGillivray, I. E. McCarthy, and M. C. Staudagi (Adam Hilger, Bristol, 1992), p. 579.
- ³⁰G. G. Balint-Kurti, F. Gögtas, S. P. Mort, A. R. Offer, A. Laganà, and O. Gervasi, J. Chem. Phys. **99**, 9567 (1993); F. Gögtas, G. G. Balint-Kurti, and A. R. Offer, *ibid.* **104**, 7927 (1996).
- ³¹M. Baer, H. J. Loesch, H.-J. Werner, and I. Last, Chem. Phys. Lett. **291**, 372 (1994); M. Baer, I. Last, and H. J. Loesch, J. Chem. Phys. **101**, 9648 (1994).
- ³²G. Villani and R. Wallace, Acta Chim. Hung. **131**, 167 (1994); ACH-Models Chem. **131**, 167 (1994).
- ³³W. Zhu, D. Wang, and J. Z. Zhang, Theor. Chem. Acc. **96**, 31 (1997).
- ³⁴M. Paniagua, A. Aguado, M. Lara, and O. Roncero, J. Chem. Phys. **109**, 2971 (1998); **111**, 6712 (1999).
- ³⁵M. Lara, A. Aguado, O. Roncero, and M. Paniagua, J. Chem. Phys. **109**, 9391 (1998).
- ³⁶F. J. Aoiz, M. T. Martinez, M. Menéndez, V. S. Rábanos, and E. Verdasco, Chem. Phys. Lett. **299**, 25 (1999).
- ³⁷F. J. Aoiz, E. Verdasco, V. S. Rábanos, H. J. Loesch, M. Menéndez, and F. Steinkemeier, Phys. Chem. Chem. Phys. **2**, 541 (2000).
- ³⁸Y. Zeiri, G. Katz, R. Kosloff, M. S. Topaler, D. G. Truhlar, and J. C. Polanyi, Chem. Phys. Lett. **300**, 523 (1999).
- ³⁹D. R. Jenkins, Proc. R. Soc. London, Ser. A **306**, 413 (1968).
- ⁴⁰M. Krauss, J. Res. Natl. Bur. Stand., Sect. A **72**, 553 (1968); K. Mizutani, T. Yano, A. Sekiguchi, K. Nayahi, and S. Muksumoto, Bull. Chem. Soc. Jpn. **57**, 3368 (1984); F. Rossi and J. Pascale, Phys. Rev. A **32**, 2657 (1985).
- ⁴¹J. C. Tully, J. Chem. Phys. **59**, 5122 (1993).
- ⁴²T. J. Martinez, Chem. Phys. Lett. **272**, 139 (1997); H. S. Lee, Y. S. Lee, and G.-H. Jeung, J. Phys. Chem. A **103**, 11080 (1999).
- ⁴³I. V. Hertel, H. Hofmann, and K. A. Rost, J. Chem. Phys. **71**, 674 (1979).
- ⁴⁴P. Botschwina, W. Meyer, I. V. Hertel, and W. Reiland, J. Chem. Phys. **75**, 5438 (1981); W. Reiland, H.-V. Tiltel, and I. V. Hertel, Phys. Rev. Lett. **48**, 1389 (1982); P. McGuire and J. C. Bellum, J. Chem. Phys. **77**, 764 (1982); N. C. Blais and D. G. Truhlar, *ibid.* **79**, 1334 (1983).
- ⁴⁵B. C. Garrett and D. G. Truhlar, in *Theory of Scattering: Papers in Honor of Henry Eyring (Theoretical Chemistry)*, edited by D. Henderson (Academic, New York, 1981), Vol. 6, Part A, p. 216.
- ⁴⁶D. G. Truhlar, J. W. Duff, N. C. Blais, J. C. Tully, and B. C. Garrett, J. Chem. Phys. **77**, 764 (1982); N. C. Blais, D. G. Truhlar, and B. C. Garrett, *ibid.* **78**, 2956 (1983).
- ⁴⁷P. Halvick and D. G. Truhlar, J. Chem. Phys. **96**, 2895 (1992).
- ⁴⁸M. D. Hack and D. G. Truhlar, J. Chem. Phys. **110**, 4315 (1999).
- ⁴⁹D. W. Schwenke, S. L. Mielke, G. J. Tawa, R. S. Friedman, P. Halvick, and D. G. Truhlar, Chem. Phys. Lett. **203**, 565 (1993); S. L. Mielke, G. J. Tawa, D. G. Truhlar, and D. W. Schwenke, J. Am. Chem. Soc. **115**, 6436 (1993); Int. J. Quantum Chem., Symp. **27**, 621 (1993); G. J. Tawa, S. L. Mielke, D. G. Truhlar, and D. W. Schwenke, J. Chem. Phys. **100**, 5751 (1994); M. D. Hack, A. W. Jasper, Y. L. Volobuev, D. W. Schwenke, and D. G. Truhlar, J. Phys. Chem. A **103**, 6309 (1999).
- ⁵⁰D. R. Yarkony, J. Chem. Phys. **84**, 3206 (1976); C. W. Eaker, *ibid.* **87**, 4532 (1987); P. Hering, S. L. Cunha, and K. L. Kompa, J. Phys. Chem. **91**, 5459 (1987); R. d. Vivie-Reidle, P. Hering, K. L. Kompa, R. R. B. Correia, S. L. Cunha, and G. Pichler, AIP Conf. Proc. **216**, 415 (1990); R. d. Vivie-Reidle, P. Hering, and K. L. Kompa, Z. Phys. D: At., Mol. Clusters **17**, 299 (1990); R. R. B. Correia, S. L. Cunha, R. d. Vivie-Reidle, G. Pichler, K. L. Kompa, and P. Hering, Chem. Phys. Lett. **186**, 531 (1991); G. Pichler, R. R. B. Correia, S. L. Cunha, K. L. Kompa, and P. Hering, Opt. Commun. **92**, 346 (1992).
- ⁵¹J. L. Magee and T. Ri, J. Chem. Phys. **9**, 639 (1941); K. J. Laidler, *ibid.* **10**, 34 (1942).
- ⁵²Y. L. Volobuev, M. D. Hack, M. S. Topaler, and D. G. Truhlar, J. Chem. Phys. **112**, 9716 (2000).
- ⁵³M. D. Hack and D. G. Truhlar, J. Chem. Phys. **114**, 2894 (2001).
- ⁵⁴M. D. Hack and D. G. Truhlar, J. Chem. Phys. **114**, 9305 (2001).
- ⁵⁵H.-D. Meyer and W. H. Miller, J. Chem. Phys. **70**, 3214 (1979).
- ⁵⁶J. C. Tully, J. Chem. Phys. **93**, 1061 (1990).
- ⁵⁷A. Bjerre and E. E. Nikitin, Chem. Phys. Lett. **1**, 179 (1967).
- ⁵⁸R. K. Preston and J. C. Tully, J. Chem. Phys. **54**, 4297 (1971); J. C. Tully and R. K. Preston, *ibid.* **55**, 562 (1971).
- ⁵⁹W. H. Miller and T. F. George, J. Chem. Phys. **56**, 5637 (1972).
- ⁶⁰J. C. Tully, in *Dynamics of Molecular Collisions*, edited by W. H. Miller (Plenum, New York, 1976), Part B, pp. 217–267.
- ⁶¹D. G. Truhlar and J. T. Muckerman, in *Atom-Molecule Collision Theory*, edited by R. B. Bernstein (Plenum, New York, 1979), pp. 505–594.
- ⁶²P. J. Kuntz, J. Kendrick, and W. N. Whitton, Chem. Phys. **38**, 147 (1979); G. Parlant and E. A. Gislason, J. Chem. Phys. **91**, 4416 (1989).
- ⁶³N. C. Blais and D. G. Truhlar, J. Chem. Phys. **79**, 1334 (1983).
- ⁶⁴M. F. Herman, J. Chem. Phys. **81**, 754 (1984).
- ⁶⁵N. C. Blais, D. G. Truhlar, and C. A. Mead, J. Chem. Phys. **89**, 6204 (1988).
- ⁶⁶P. J. Kuntz, J. Chem. Phys. **95**, 141 (1991).
- ⁶⁷S. Chapman, Adv. Chem. Phys. **82**, 423 (1992).
- ⁶⁸M. F. Herman, Annu. Rev. Phys. Chem. **45**, 83 (1994).
- ⁶⁹U. Müller and G. Stock, J. Chem. Phys. **107**, 6230 (1997).
- ⁷⁰J. C. Tully, in *Modern Methods for Multidimensional Dynamics Computations in Chemistry*, edited by D. L. Thompson (World Scientific, Singapore, 1998), p. 34.
- ⁷¹M. D. Hack and D. G. Truhlar, J. Phys. Chem. A **104**, 7917 (2000).
- ⁷²A. W. Jasper, M. D. Hack, and D. G. Truhlar, J. Chem. Phys. **115**, 1804 (2001).
- ⁷³A. W. Jasper, M. D. Hack, D. G. Truhlar, and P. Piecuch (to be published).
- ⁷⁴R. J. Buenker and S. D. Peyerimhoff, Theor. Chim. Acta **35**, 33 (1974).
- ⁷⁵R. J. Buenker and S. D. Peyerimhoff, Theor. Chim. Acta **39**, 217 (1975).
- ⁷⁶P. J. Bruna and S. D. Peyerimhoff, Adv. Chem. Phys. **67**, 1 (1987).
- ⁷⁷A. D. McLachlan, Mol. Phys. **4**, 417 (1961).
- ⁷⁸T. F. O'Malley, Adv. At. Mol. Phys. **7**, 223 (1971).
- ⁷⁹V. Sidis and H. Lefebvre-Brion, J. Phys. B **4**, 1040 (1971).
- ⁸⁰S. A. Evans, J. S. Cohen, and N. F. Lane, Phys. Rev. A **4**, 2235 (1971).
- ⁸¹R. W. Numrich and D. G. Truhlar, J. Phys. Chem. **79**, 2745 (1975).
- ⁸²A. Macias and A. Riera, J. Phys. B **11**, L489 (1978).
- ⁸³C. A. Mead and D. G. Truhlar, J. Chem. Phys. **77**, 6090 (1982).
- ⁸⁴C. A. Mead, J. Chem. Phys. **78**, 807 (1983).
- ⁸⁵T. C. Thompson, D. G. Truhlar, and C. A. Mead, J. Chem. Phys. **82**, 2392 (1985).
- ⁸⁶V. Sidis, Adv. Chem. Phys. **82**, 73 (1992).
- ⁸⁷T. Pacher, L. S. Cederbaum, and H. Köppel, Adv. Chem. Phys. **84**, 293 (1993).
- ⁸⁸V. M. García, M. Reguero, R. Caballol, and J. P. Malrieu, Chem. Phys. Lett. **281**, 161 (1997).
- ⁸⁹G. J. Atchity and K. Ruedenberg, Theor. Chem. Acc. **97**, 47 (1997).
- ⁹⁰M. D. Hack, A. W. Jasper, Y. L. Volobuev, D. W. Schwenke, and D. G. Truhlar, J. Phys. Chem. A **103**, 6309 (1999).
- ⁹¹Genetic algorithm calculations were carried out using the program FORTRAN GA, version 1.6.4 as described in D. L. Carroll, AIAA J. **34**, 338 (1996).
- ⁹²See EPAPS Document No. E-JCPSA6-115-008141 for supporting information including the functional forms and parameters of the analytic LiFH and NaFH-B surface sets. This document may be retrieved via the EPAPS homepage (<http://www.aip.org/pubservs/epaps.html>) or from <ftp.aip.org> in the directory /epaps/. See the EPAPS homepage for more information.
- ⁹³M. S. Topaler, M. D. Hack, Y. L. Volobuev, A. W. Jasper, T. C. Allison, T. F. Miller III, Y.-P. Liu, N. C. Blais, and D. G. Truhlar, NAT-version 6.4 (University of Minnesota, Minneapolis, 2001).
- ⁹⁴E. B. Wilson, J. C. Decius, and P. C. Cross, *Molecular Vibrations* (McGraw-Hill, New York, 1955).
- ⁹⁵J. C. Corchado, Y.-Y. Chuang, P. L. Fast *et al.*, POLYRATE-version 8.5.1, University of Minnesota, Minneapolis, 2000.
- ⁹⁶A. D. Isaacson and D. G. Truhlar, J. Chem. Phys. **76**, 1380 (1982).
- ⁹⁷M. S. Topaler, T. C. Allison, D. W. Schwenke, and D. G. Truhlar, J. Chem. Phys. **109**, 3321 (1998).